

An improved pushover analysis procedure for multi-mode seismic performance evaluation of bridges: (2) Correlation study for verification

Kwak, Hyo-Gyoung[†] and Shin, Dong Kyu[‡]

Department of Civil and Environmental Engineering, Korea Advanced Institute of Science and Technology,
373-1 Guseong-dong, Yuseong-gu, Daejeon 305-701, Korea

(Received January 29, 2009, Accepted August 13, 2009)

Abstract. In the companion paper, a simple but effective analysis procedure termed an Improved Modal Pushover Analysis (IMPA) is proposed to estimate the seismic capacities of multi-span continuous bridge structures on the basis of the modal pushover analysis, which considers all the dynamic modes of a structure. In contrast to previous studies, the IMPA maintains the simplicity of the capacity-demand curve method and gives a better estimation of the maximum dynamic response in a bridge structure. Nevertheless, to verify its applicability, additional parametric studies for multi-span continuous bridges with large differences in the length of adjacent piers are required. This paper, accordingly, concentrates on a parametric study to review the efficiency and limitation in the application of IMPA to bridge structures through a correlation study between various analytical models including the equivalent single-degree-of-freedom method (ESDOF) and modal pushover analysis (MPA) that are usually used in the seismic design of bridge structures. Based on the obtained numerical results, this paper offers practical guidance and/or limitations when using IMPA to predict the seismic response of a bridge effectively.

Keywords: bridges; improved modal pushover; seismic performance; parametric study; A-D relation.

1. Introduction

An increase of the importance of the seismic design of multi-span continuous bridges and/or multi-story buildings requires more understanding of the inelastic behavior of such structures, as strong ground motions usually cause large deformations with severe damage at critical regions such as the bottom face of piers in bridges and the beam-to-column joints in buildings. In particular, to evaluate seismic design requirements related to the prevention of a structural collapse, inelastic analyses considering the nonlinearity due to the sequential development of plastic hinges must be conducted (Lawson *et al.* 1994). However, as the nonlinear behavior of a structure makes it impossible to adopt the principle of superposition in the dynamic analysis, designation of a general method that can be applied to the structures with multi-degree-of-freedom remains difficult (Krawinkler and Seneviratna 1998); thus, the performance-based seismic design (PBSD) has been

[†] Professor, Corresponding author, E-mail: khg@kaist.ac.kr

[‡] Doctoral Course Student, E-mail: dongkyu.shin@gmail.com

introduced as an alternative method (Chopra and Goel 2002).

A major challenge to the PBSO, however, is to develop simple and effective methods for designing, analyzing and checking the designs of structures so that they reliably meet selected performance objectives. In response to this need, several simplified nonlinear analysis procedures that determine the displacement demand in PBSO were incorporated in the ACT-40 (1996) and FEMA-274 (1997) documents. However, several deficiencies in these methods exist. Numerous iterations are required to reach the final performance point in which the capacity and demand diagrams are intersect each other; moreover, the iterative procedure may not give a converged result in some cases. Accordingly, Freeman (1998) and Chopra et al. introduced an improved capacity spectrum method (Chopra and Goel 2004). More details related to this method can be found in the literature (Chopra and Goel 2001).

As mentioned in the companion paper, the key issue in the capacity spectrum diagram method centers on the determination of a representative capacity curve for an equivalent single-degree-of-freedom in multiple-degree-of-freedom structures. The modal pushover analysis (MPA) was introduced by Chopra *et al.* (Chopra and Goel 2002) on the basis of structural dynamic theory and has been popularly used in seismic analyses of building structures. In addition, an improved modal pushover analysis (IMPA) is introduced in the companion paper for a more effective application of the modal pushover analysis of multi-span continuous bridges, Its exactness is also validated in an application to three representative bridges. However, an evaluation of the seismic performance of the introduced method (IMPA) should be conducted through additional parametric studies that can verify its applicability and review its limitations.

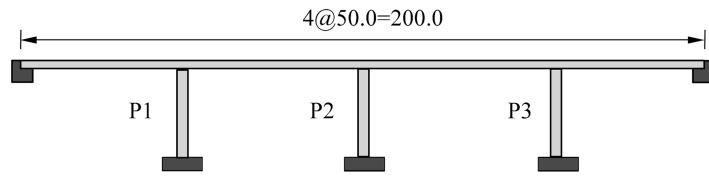
This paper, therefore, concentrates on parametric studies of bridges with changes in their design variables that affect the structural stiffness of the bridges (such as the bending stiffness ratio of the super-structure to sub-structure and the pier length). On the basis of the obtained numerical results, the structural behavior of multi-span continuous bridges subjected to earthquake loading can be analyzed, and guidance toward reliable results regardless of changes in the bridge stiffness is specified quantitatively with the introduced method.

2. Example bridges

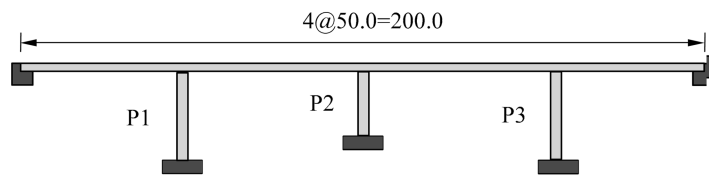
Numerical analyses were conducted for the six bridges shown in Fig. 1 with different configurations in the bending stiffness of the sub-structure. Representative cross-section geometries for the super-structure (deck) and sub-structure (pier) are shown in Fig. 2. In addition, the bending stiffness ratio of the sub-structure to the super-structure is defined by Eq. (1), and seven variations of D (1, 5, 10, 50, 100, 200, and 500) were selected on the basis of the change in the length of the piers. Thus, a total of 42 different bridges were designed according to the combination of the bending stiffness ratio and the configuration of the bridge.

$$D = \frac{\sum K_p}{K_D} \quad (1)$$

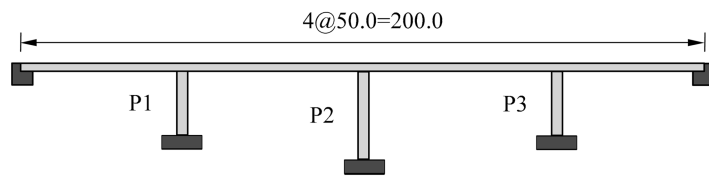
Here, the bending stiffness of pier i is $K_p = 3E_{p_i}I_{p_i}/L_{p_i}^3$, the bending stiffness of the deck is $K_D = 48E_D I_D / L_D^3$, EI denotes the bending stiffness of a section in the transverse direction, L_{p_i} is the length of pier i , and L_D is the total length of the bridge ($L_D = 200$ m in this paper).



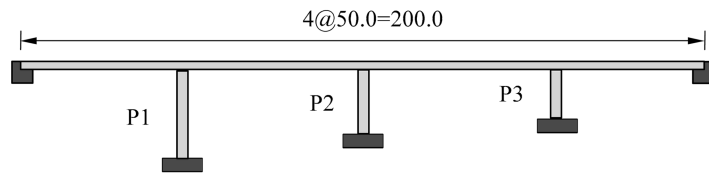
(a) B111 ($K_{p1} = K_{p2} = K_{p3}$ case)



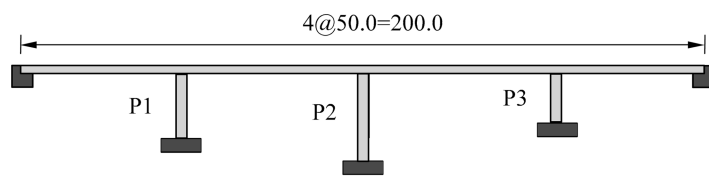
(b) B131 ($K_{p1} = K_{p3} = \frac{1}{3} K_{p2}$ case)



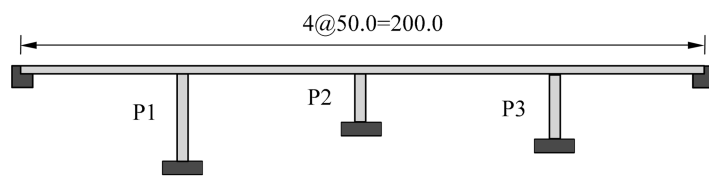
(c) B313 ($K_{p1} = K_{p3} = 3K_{p2}$ case)



(d) B135 ($K_{p1} = \frac{1}{3} K_{p2} = \frac{1}{5} K_{p3}$ case)



(e) B315 ($K_{p1} = 3K_{p2} = \frac{3}{5} K_{p3}$ case)



(f) B153 ($K_{p1} = \frac{1}{5} K_{p2} = \frac{1}{3} K_{p3}$ case)

Fig. 1 Geometric configuration of example structures (unit:m)

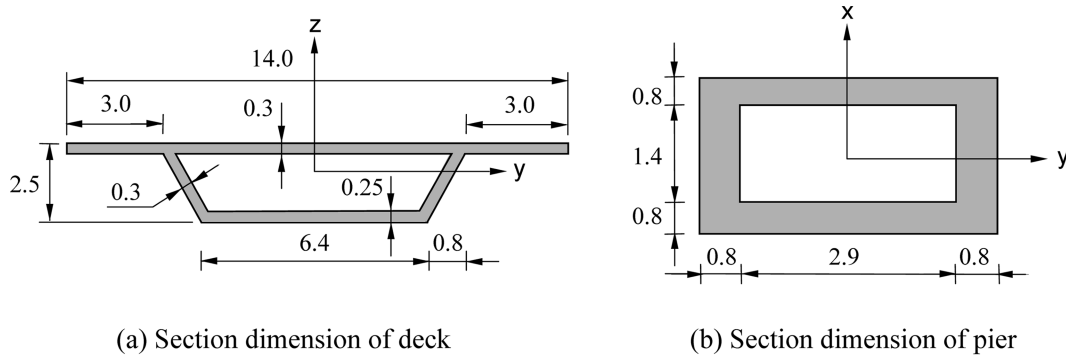


Fig. 2 Section dimensions in bridge (unit:m)

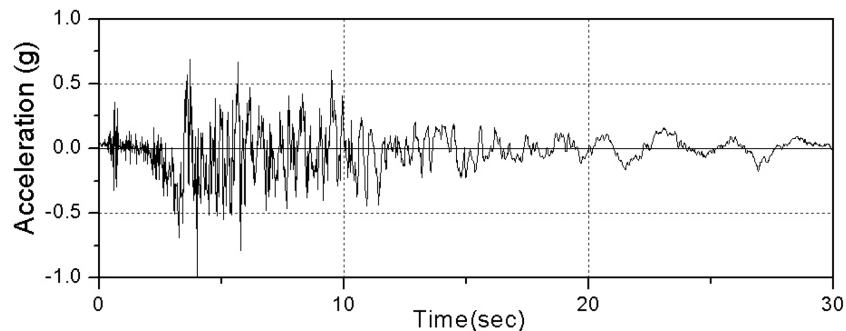
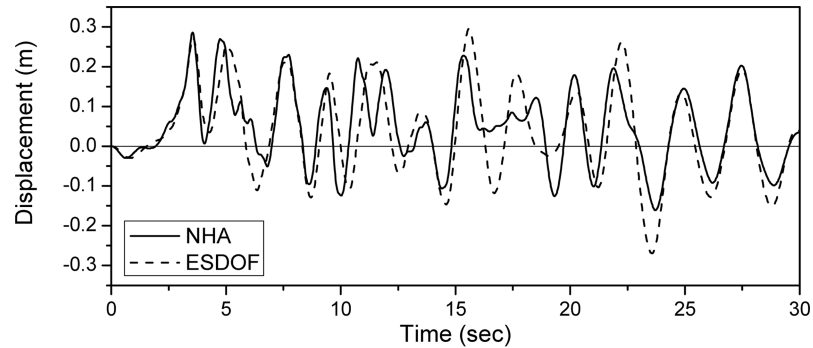


Fig. 3 Ground motion of Northridge 1.0G

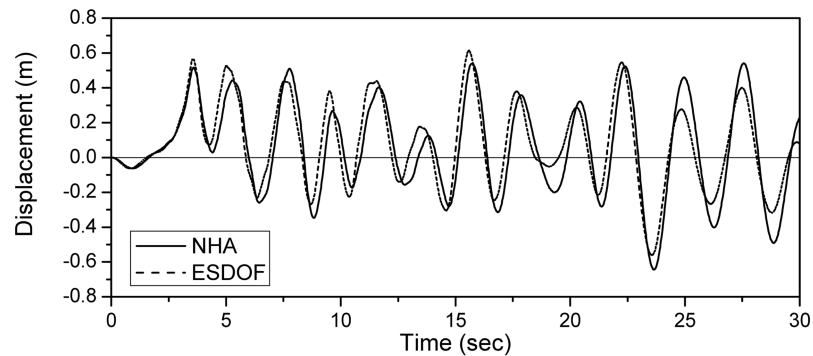
As shown in Fig. 1, three bridge types of B111, B131 and B313 represent a symmetric bridge configuration, while the other types (B135, B315 and B153) show an asymmetric bridge configuration. The numbers used in defining a bridge indicate the relative bending stiffness ratios of each pier, as can be shown in Fig. 1. In particular, inelastic numerical analyses may depend on the relative bending stiffness of the super-structure to the sub-structure. To be coincident with the frequently used ratios in designs, accordingly, the bending stiffness ratio D defined in Eq. (1) is assumed to range from 1 to 500 through an investigation of numerous small-to-medium span bridges constructed in practice.

A nonlinear modal pushover analysis and nonlinear time history analysis (NHA) (Nawrocki 2009) for the example structures were conducted using the OpenSees version 1.6.2 software (OpenSees Development Team 1998-2002), and the results obtained from the NHA were used as the reference values for comparing the results by three different approaches of the equivalent single degree-of-freedom method (ESDOF), the modal pushover analysis (MPA), and the improved modal pushover analysis (IMPA). Moreover, the Northridge earthquake data (EQ 4) in Fig. 3 was used to generate an artificial ground motion with a maximum ground acceleration of 1.0G on the basis of the elastic seismic response spectrum defined in a design code (Ministry of Construction and Transportation 2000).

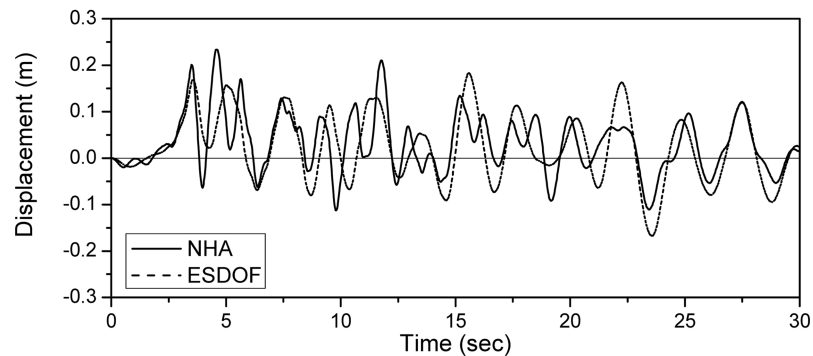
As reviewed in the companion paper, to discuss the applicability and limitations in use, comparisons between the three representative methods of ESDOF, MPA and IMPA were also



(a) Time history response of Pier 1



(b) Time history response of Pier 2



(c) Time history response of Pier 3

Fig. 4 Time history response of B135 with $D = 100$ using ESDOF

conducted for a typical bridge of B135 with $D = 100$, which shows stronger asymmetricity between the piers and a larger stiffness ratio between the sub-structure and the super-structure compared to bridge B32 in the companion paper. All of the procedures conducted for the time history analysis based on the A-D relationship are identical to those used in the companion paper, and the obtained time history responses of bridge B135 with D100 in the three different approaches of ESDOF, MPA and IMPA are shown in Figs. 4, 5, and 6. These numerical results show that the obtained conclusions in the companion paper have been consistently maintained, and that the introduced

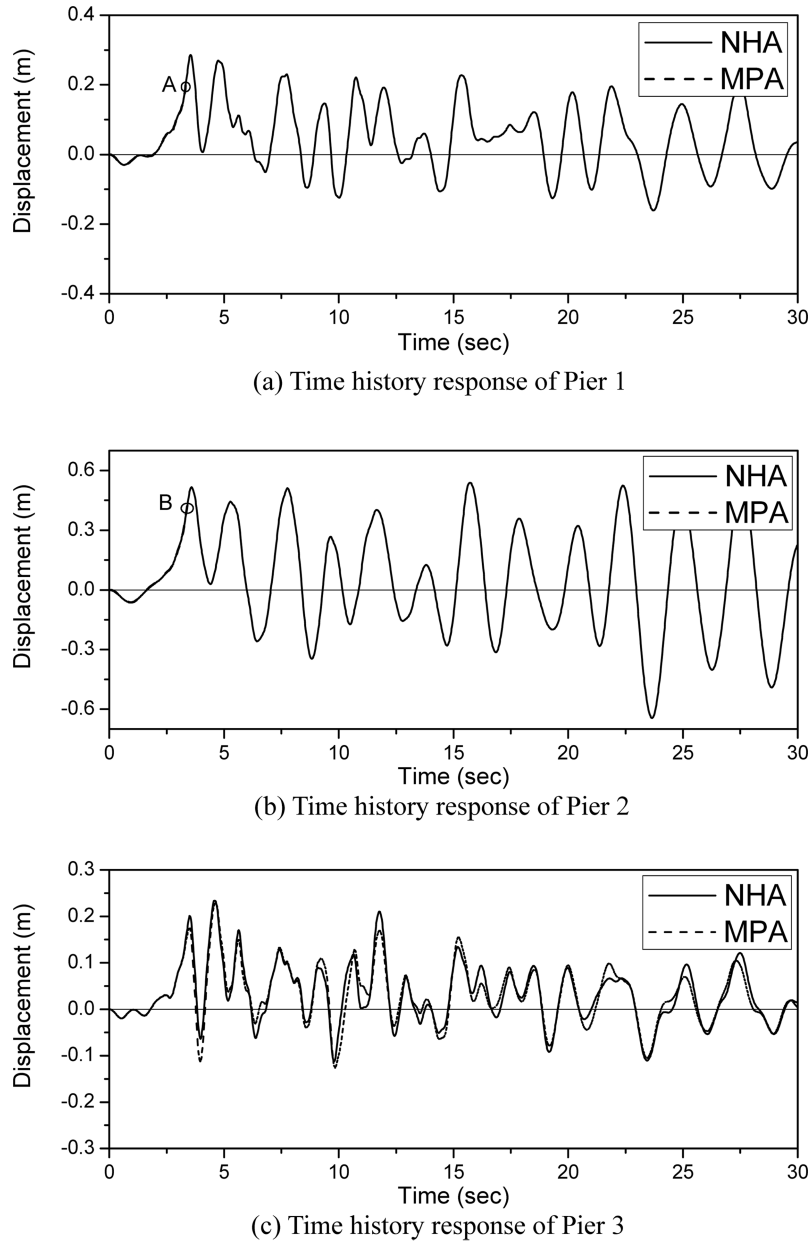


Fig. 5 Time history response of B135 with D100 using MPA

method (IMPA) can still be used effectively, even in a bridge with strong asymmetry. On the other hand, the calculation of the time-histories for the displacement response at the top of the piers is likely unworkable using a conventional modal pushover analysis (MPA) (see circles A and B in Figs. 5(a) and 5(b)), as the A-D relationships constructed at Piers 1 and 2 represent a displacement reversal, as is shown in Fig. 11 in the companion paper.

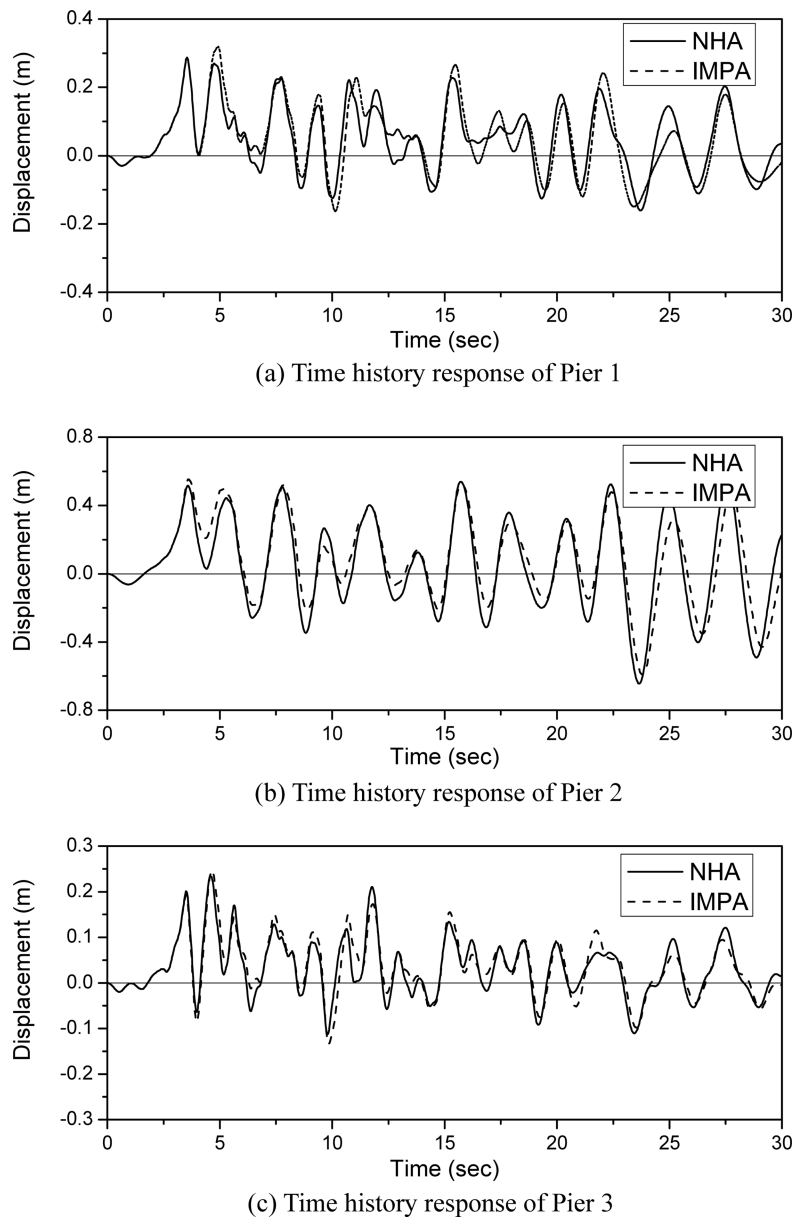


Fig. 6 Time history response of B135 with D100 using IMPA

3. Calculation of the relative error

When bridge B135 with D100 was subjected to the ground motion defined in Fig. 3, its maximum structural response can be predicted not only by a nonlinear time history analysis but also by the capacity spectrum method. The maximum lateral displacements calculated by the latter method are shown in Figs. 7 to 9 for the three different approaches, respectively. Naturally, determination of the demand curve that satisfies the ductility μ also requires an iterative calculation of the nonlinear

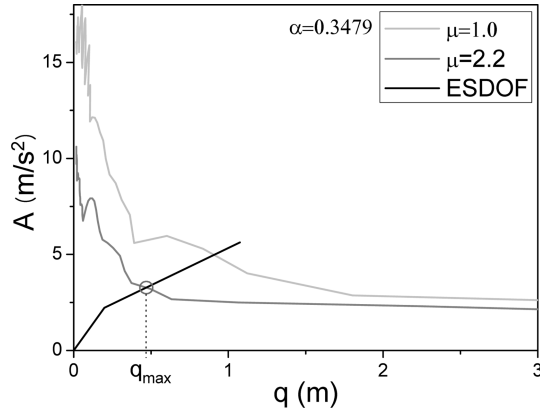
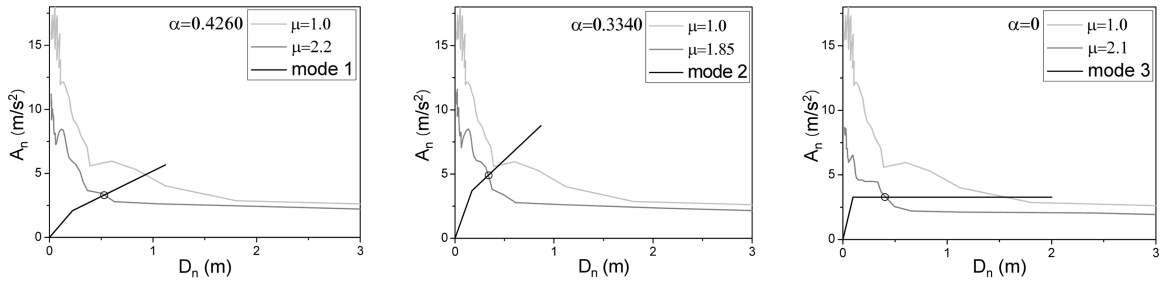
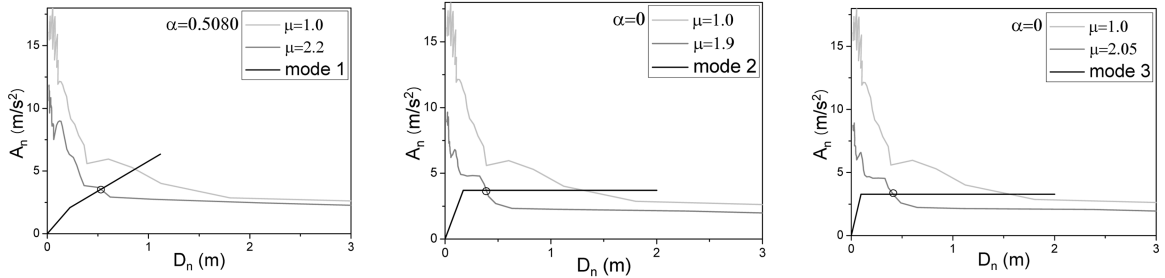


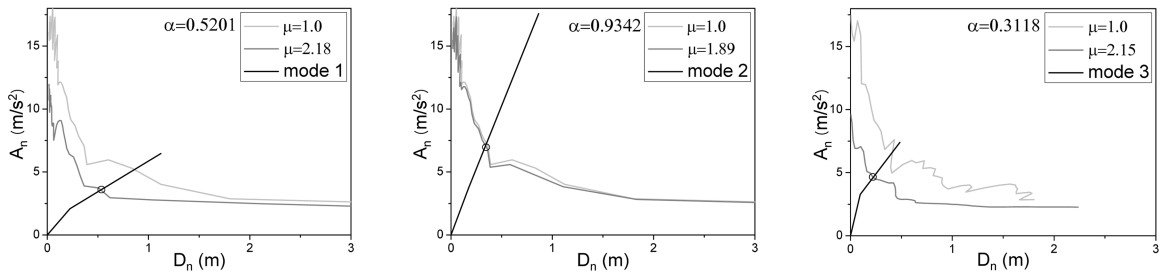
Fig. 7 Capacity spectrum method using ESDOF in B135 with $D = 100$



(a) 1st, 2nd and 3rd vibration mode of Pier 1



(b) 1st, 2nd and 3rd vibration modes of Pier 2



(c) 1st, 2nd and 3rd vibration mode of Pier 3

Fig. 8 Capacity spectrum method using MPA in B135 with $D = 100$

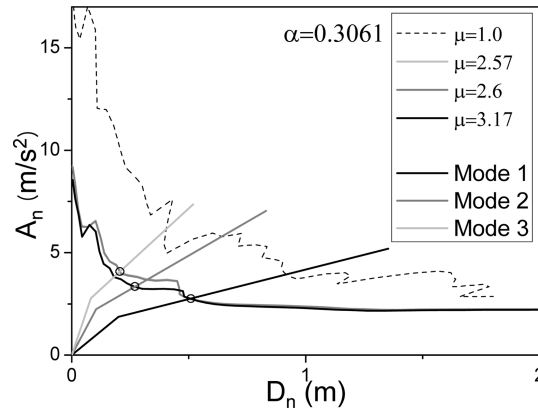


Fig. 9 Capacity spectrum method using IMPA in B135 with D = 100

Table 1 Maximum displacement estimation using the capacity spectrum method in B135 with D = 100

Pier	NHA	ESDOF	MPA	IMPA
	$(U_{\text{pier}})_{\text{max}}$	$(U_{\text{pier}})_{\text{max}}$	$(U_{\text{pier}})_{\text{max}}$	$(U_{\text{pier}})_{\text{max}}$
1	0.2856 m	0.2825 m	0.2588 m	0.2683 m
2	0.6443 m	0.5876 m	0.5911 m	0.6288 m
3	0.2339 m	0.1755 m	0.2046 m	0.2071 m

Table 2 Error rates of estimation using the capacity spectrum method in B135 with D = 100

Pier	ESDOF error rate	MPA error rate	IMPA error rate
1	1.1%	9.38%	6.07%
2	8.8%	8.26%	2.41%
3	24.99%	12.53%	11.45%

seismic response spectrum, and the maximum lateral displacement corresponds to the point where the capacity curve intersects the demand curve. The calculation of the expected maximum lateral displacement $\{u\}$ for each pier is done using Eq. (3) in the companion paper; its obtained results are summarized in Table 1, in which NHA can be used as the reference values because these values are obtained from a rigorous nonlinear time history analysis of the entire structure without any simplification. Particularly, the displacement reversals in the A-D relationship typically appearing in the case of MPA are ignored by introducing an arbitrary assumption of perfect plastic behavior at the post-yielding stage to conduct the nonlinear analysis by the time history analysis and/or the capacity spectrum method, as was discussed in the companion paper. Table 2, representing the relative errors in the calculated maximum lateral displacement to those obtained by the NHA (see Eq. (13) in the companion paper) also shows that the introduced method IMPA gives more reliable results than the ESDOF and MPA methods.

In order to reach a generalized conclusion, additional parametric studies of bridges with different compositions in their bending stiffness must be conducted. The 42 bridges in Fig. 2 were analyzed, and the results obtained from nonlinear time history analyses (NHA) of the bridges are compared in

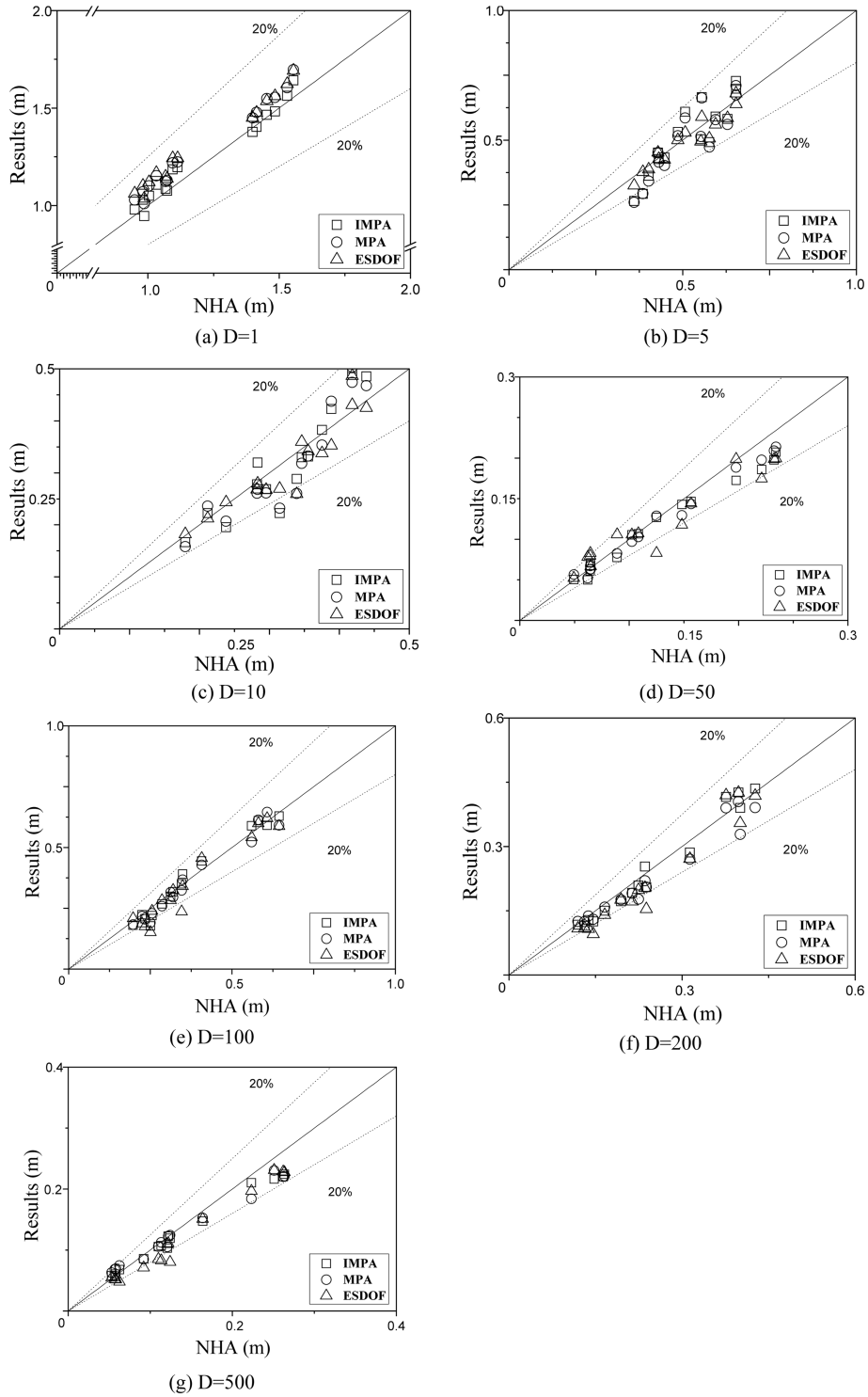


Fig. 10 Results of three different capacity spectrum methods for 42 bridges under Northridge 1.0G

Table 3 Error rates according to the change in the stiffness ratio (D)

D	Analysis Method	Average Error rate	Maximum Error rate
1	ESDOF	8.765%	13.520%
	MPA	7.244%	11.685%
	IMPA	3.559%	8.315%
5	ESDOF	5.229%	12.257%
	MPA	10.927%	27.796%
	IMPA	9.958%	26.396%
10	ESDOF	6.802%	23.531%
	MPA	11.533%	26.333%
	IMPA	10.638%	29.227%
50	ESDOF	14.617%	33.533%
	MPA	7.430%	15.999%
	IMPA	7.731%	19.845%
100	ESDOF	10.475%	39.542%
	MPA	7.860%	23.903%
	IMPA	7.551%	29.152%
200	ESDOF	15.280%	35.419%
	MPA	9.608%	21.268%
	IMPA	8.435%	14.352%
500	ESDOF	14.867%	35.310%
	MPA	10.959%	20.693%
	IMPA	8.356%	15.955%

Fig. 10 together with the results from ESDOF, MPA and IMPA. The earthquake data of Northridge 1.0G was used here as well, and the maximum lateral displacement developed in a given bridge was taken as the reference value. As shown in Fig. 10, most cases lie in the range with a maximum error of 20%, which is believed to be within an acceptable accuracy range. Table 3 also summarizes the average error at all piers and the maximum error developed at a pier in an arbitrary bridge for each stiffness ratio D.

From Fig. 10 and Table 3, the following results can be inferred. When the stiffness ratio D is small, implying that the stiffness of the super-structure is relatively strong, all of the pushover analysis-based results give very close predictions to those by the NHA. However, as the stiffness ratio increases in proportion to the increase in the bending stiffness in the sub-structure, the relative differences in the maximum lateral displacement between the NHA and the pushover analyses of ESDOF, MPA and IMPA increase. However, the maximum difference in each analysis does not occur in the case of the largest stiffness ratio of D = 500. The reason for these relative error variations depending on the stiffness ratio can be inferred from the theoretical background of the capacity spectrum method. Specifically, the relative error occurred from the adopted basic assumption that the deformation shape of the bridge (see ϕ_n in Eq. (4) in the companion paper) obtained within the elastic deformation boundary is maintained even at the post-yielding stage.

Table 3 also shows that ESDOF, which is the simplest method among the ESDOF, MPA and IMPA approaches, can be used effectively when the stiffness ratio is relatively small. In this case,

however, its accuracy gradually decreases as the stiffness ratio increases. On the other hand, the introduced IMPA approach, which is simple in spite of that fact that it considers all of the vibration modes, maintains its accuracy within an acceptable relative error range regardless of the increase and/or decrease of the stiffness ratio. And it is easily shown that IMPA gives as good results as conventional MPA.

4. Applicability of IMPA

As reviewed previously, IMPA gives more accurate results compared to ESDOF and MPA for predictions of the maximum lateral displacements of bridges while maintaining its simplicity of application. However, the accuracy may be low within some ranges of stiffness ratio D , implying that additional parametric studies for IMPA may be required to determine if any limitation exist in use and then to propose a guideline to reserve the accuracy in numerical analyses. The six bridges mentioned in Fig. 2 are used without any modification and the seven stiffness ratios assumed in this paper are also used. Basically, the stiffness ratio can be changed by adjusting the bending stiffness of the super-structure or that of the sub-structure through changes in the span length or in the height of the pier, respectively. As both procedures for changing the bending stiffness are adopted, the number of example structures to be analyzed becomes 84. In addition, the additional artificial seismic data of Elcentro 1.0G and San Fernando 1.0G shown in Figs. 11 and 12, respectively, were also used in the following parametric studies. The obtained results are summarized in Fig. 13 and Table 4.

An important feature of the data shown in Fig. 13 and Table 4 is that the accuracy of IMPA depends on the relative ratio of the bending stiffness between the super-structure and the sub-

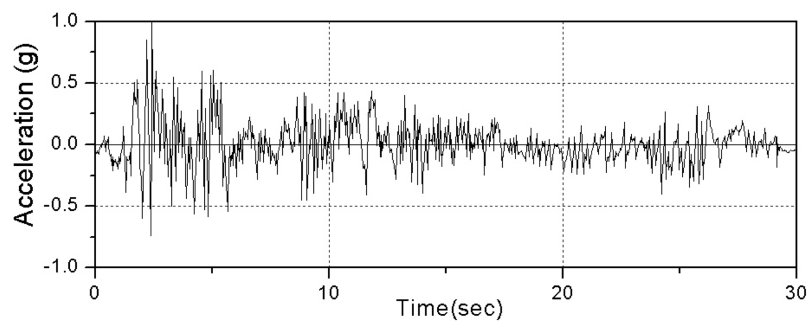


Fig. 11 Ground motion of Elcentro 1.0G

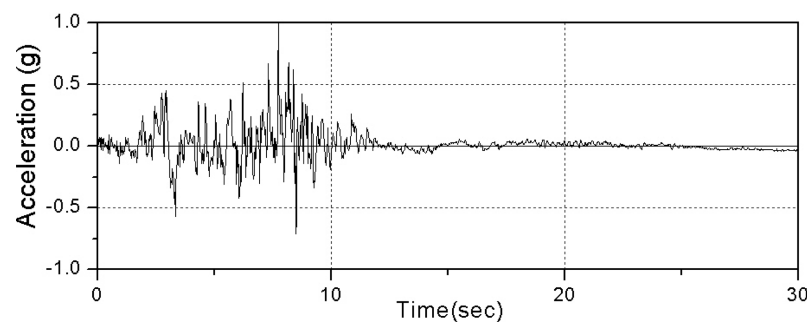


Fig. 12 Ground motion of San Fernando 1.0G

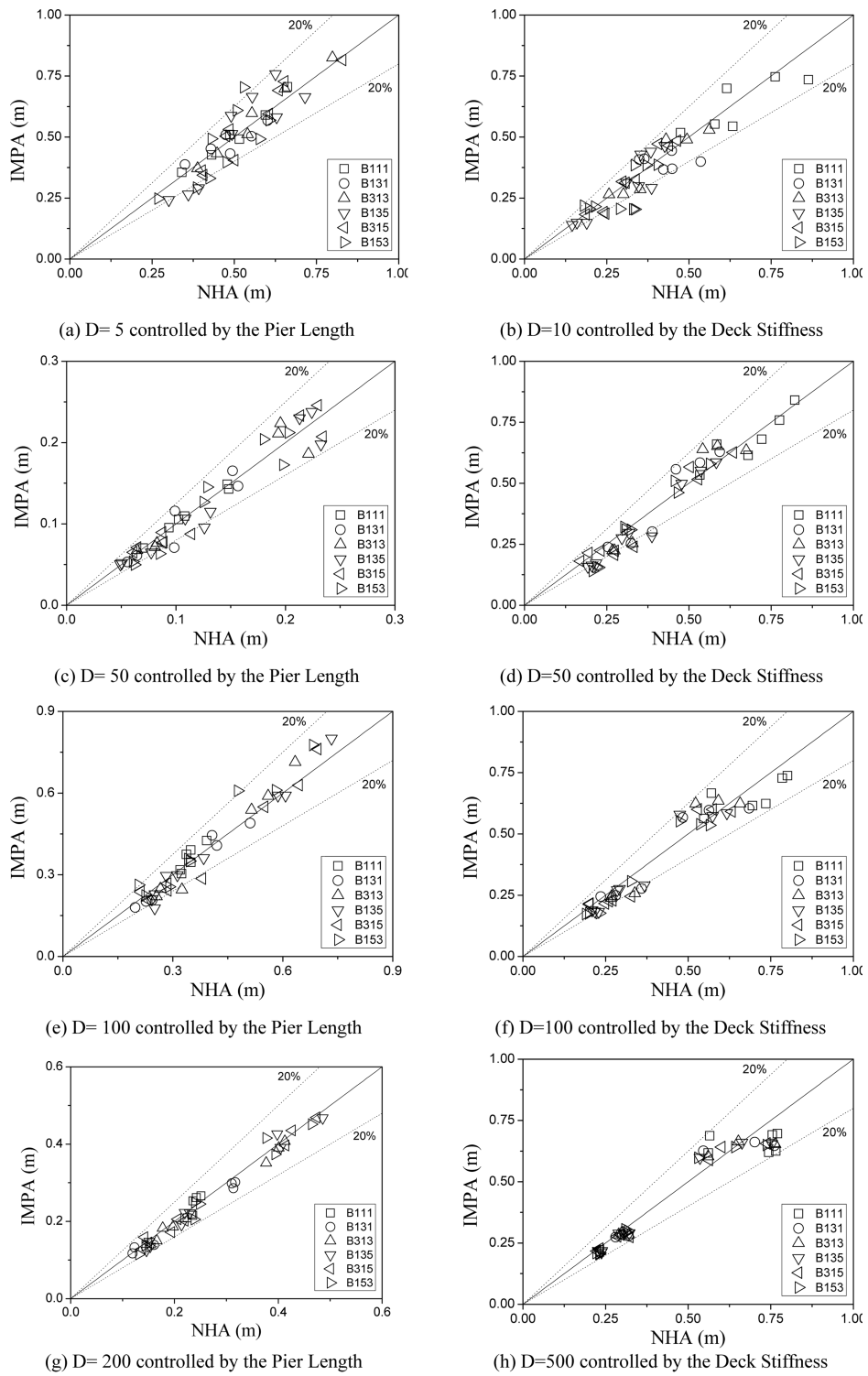


Fig. 13 Results of IMPA for 84 bridges in three earthquakes

Table 4 Error rates according to the change in the stiffness ratio (D)

D	Stiffness Control Method	Average Error rates	Maximum Error rates
1	Pier length (K_p)	3.09%	9.10%
	Deck Stiffness (K_D)	3.72%	14.30%
5	Pier length (K_p)	10.08%	33.00%
	Deck Stiffness (K_D)	8.33%	25.70%
10	Pier length (K_p)	10.95%	33.80%
	Deck Stiffness (K_D)	11.99%	34.20%
50	Pier length (K_p)	9.07%	28.00%
	Deck Stiffness (K_D)	12.05%	32.00%
100	Pier length (K_p)	9.10%	29.20%
	Deck Stiffness (K_D)	11.26%	25.20%
200	Pier length (K_p)	6.36%	14.40%
	Deck Stiffness (K_D)	10.75%	25.30%
500	Pier length (K_p)	6.14%	16.00%
	Deck Stiffness (K_D)	8.52%	21.70%

structure rather than on the magnitude of the absolute value of the bending stiffness. In addition, the obtained results represent the similar errors for each bending stiffness ratio regardless of the change in the stiffness ratio with the bending stiffness of the super-structure (K_p controlled in Table 4) or with that of the sub-structure (K_D controlled in Table 4). However, in contrast to the average error for the three piers, the maximum error occurring at a pier shows a difference of more than 30% from NHA when the stiffness ratios ranged from $D = 5$ to $D = 50$. However these large error rates are contributed by truncational error in small displacement. These large differences appear to have been caused by the asymmetric configuration of the bridge, as induced from the difference in the height of adjacent piers. Nevertheless, the structural responses in the bridge structure evaluated from IMPA maintain higher accuracy than those obtained from ESDOF and MPA.

The maximum and averaged errors listed in Table 4 are also graphically represented in Fig. 14, and the maximum errors of these values in each bridge type are shown in Table 5. This table

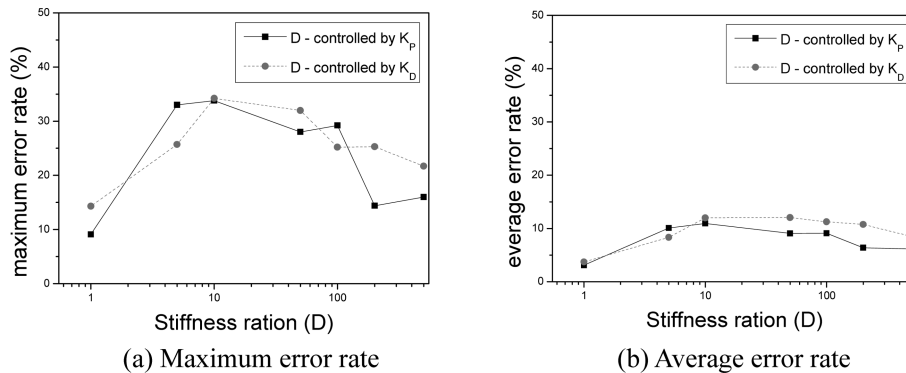


Fig. 14 IMPA Error rates according to the stiffness ratio (D)

Table 5 Error rates in bridges

Bridge Shape	Average Error rates	Maximum Error rates
B111	6.66%	25.30%
B131	10.21%	32.10%
B313	8.38%	24.50%
B135	10.12%	32.70%
B315	8.64%	31.70%
B153	12.54%	34.20%

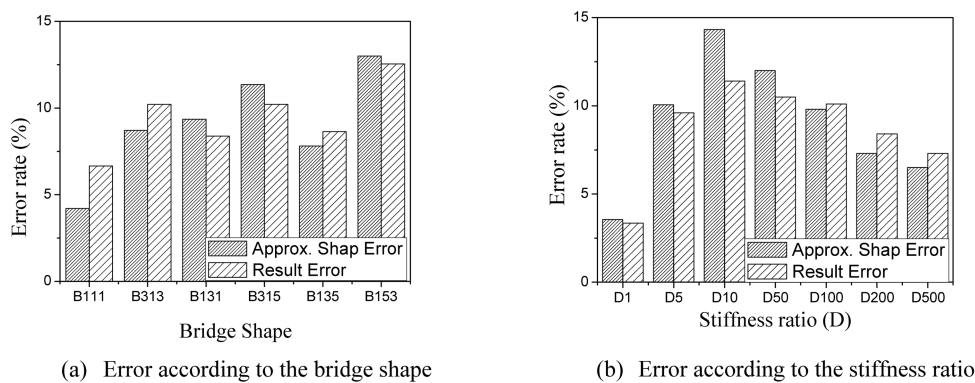


Fig. 15 Relationship between shape error and result error

indicates that the accuracy also depends on the degree of symmetry of the bridges as well as on the stiffness ratio. In spite of the same degree of symmetry, however, bridge B313 shows a more accurate result than bridge B131, which implies that bridges in which the first vibration mode is simply considered experience relatively small errors. Specifically, the relatively short length of the center pier in bridge B131 makes it difficult to reflect the dominant first vibration mode. A similar conclusion can also be inferred in bridges B315 and B135. Accordingly, the accuracy of IMPA depends on the bridge type as well as the stiffness ratio due to the adopted assumption that the deformation determined in the elastic stage is maintained even after the yielding of the piers (Fig. 5 in the companion paper).

Fig. 15 compares the maximum shape errors with the average displacement errors between NHA and IMPA with respect to the stiffness ratio and the bridge shapes, where the shape error indicates the summation of the difference between U_{pier} and $U_{a, pier}$ in Fig. 5 in the companion paper. The average displacement errors are those shown in Tables 4 and 5. The following can also be inferred from Fig. 15: (1) the accuracy of IMPA has a strong correlation with the deformation shape assumed, (2) the stiffness ratios ranging from $D = 10$ to $D = 50$ show remarkable differences in the shape error together with those in the displacement error, and (3) as the degree of symmetry in bridge shapes also affect the shape error, a more reliable result can be expected with greater bridge symmetry.

5. Conclusions

The companion paper proposes an improved modal pushover analysis method to evaluate the

seismic performance of multi-span continuous bridges effectively while the present paper concentrates on the additional parametric studies to verify the efficiency and applicability and introduces guidance for the application of IMPA regardless of the bridge configuration. From these parametric studies, the following conclusions were made: (1) the introduced IMPA method is more effective compared to the ESDOF and MPA methods for a seismic analysis of bridge structures, because the IMPA method typically gives similar or even more accurate solution regardless of the bridge configuration and applied earthquake loading; (2) given that the proposed method requires only one pushover analysis and one set of demand curves while considering all vibration modes, its application is relatively simple. However, it is also true that a number of limitations exist in its application to nonsymmetrical bridges; (3) when the shape error representing the difference in the displacements of bridge before and after the yielding of the sub-structure is larger than 10%, an application of IMPA may not give a feasible result, even when the developed error in the seismic response of the bridge is smaller than that determined by ESDOF or MPA; (4) the accuracy of the IMPA results may not be reserved if the stiffness ratio ranges from 10 to 50; (5) in bridge structures with stiffness ratios of larger than 50 or less than 10, the IMPA can be effectively used while maintaining error rates at all piers of less than 20%, regardless of the degree of symmetry in the bridge configuration. However, if the stiffness ratio ranges from 10 to 50, the IMPA can only be applied to bridges with high symmetry. (6) Finally, the introduced IMPA method is expected to be used effectively in real bridge structures, because in contrast to the 42% difference in the stiffness ratio between two adjacent piers that is assumed in the parametric study, most bridge structures in practice do not have a difference larger than 20% in the stiffness ratios between two adjacent piers. Nevertheless, to offer a more rational approach, extensive studies for reliability should be conducted. Before the introduced method is applied to a highly nonsymmetrical bridge, additional rigorous time history analysis must be conducted in order to verify the accuracy of the obtained results.

Acknowledgements

This research was supported by a grant (07High Tech A01) from High tech Urban Development Program funded by Ministry of Land, Transportation and Maritime Affairs of Korean government and from the Smart Infra-Structure Technology Center funded by the Korea Science and Engineering Foundation.

References

- Chopra, A.K. (2001), "Dynamics of structures: Theory and application to earthquake engineering", Prentice-Hall: Englewood Cliffs, NJ.
- Chopra, A.K. and Goel, R.K. (2002), "A modal pushover analysis procedure for estimating seismic demands for buildings.", *Earthq. Eng. Struct. Dyn.*, **31**, 561-582.
- Chopra, A.K. and Goel, R.K. (2004), "A modal pushover analysis procedure to estimate seismic demands for unsymmetric-plan buildings.", *Earthq. Eng. Struct. Dyn.*, **33**, 903-927.
- Freeman, S.A. (1998), Development and Use of Capacity Spectrum Method, Proceedings of 6th U.S. National Conference on Earthquake Engineering. Seattle, EERI, Oakland, California.
- Krawinkler, H. and Seneviratna, G.D.P.K. (1998), "Pros and cons of a pushover analysis of seismic performance

- evaluation”, *Eng. Struct.*, **20**(4-6), 452-464.
- Lawson, R.S., Vance, V. and Krawinkler, H. (1994), “Nonlinear static pushover analysis-why, when and how?”, *Proceedings of the 5th U.S. Conf. Earthq. Eng.*, **1**, 283-292.
- Ministry of Construction and Transportation (2000), Standard Specification for Highway Bridges. 2nd ed., Korea Road & Transportation Association.
- Nawrocki, P.A. (2009), “Alterations of breakdown and collapse pressures due to material nonlinearities”, *Geomech. Eng.*, **1**(2), 155-168.
- OpenSees Development Team (1998-2002), OpenSees: Open System for Earthquake Engineering Simulation, <http://opensees.berkeley.edu/>, Pacific Earthquake Engineering Research Center, University of California, Berkeley, CA.